Importance of the applied compression on the tumor sliding behavior in ultrasound axial-shear strain image

Belfor Galaz and Esteban Donoso
Departamento de Física, Universidad de Santiago de Chile,
Av. Ecuador 3493, Casilla 307, Correo 2, Santiago, Chile.
(Dated: July 26, 2018)

The rotation Fill-in is a benignity signature presents on Rotation Elastogram (RE) that may be used for breast tumor classification during freehand ultrasound quasi-static elastography scanning. It came from the bounding condition at the interface between the tumor and surrounding host tissue that in the case of benign lesions, which is generally loosely bounded, induces its rotation when is submitted to asymmetric stress distribution along the lateral direction. This last is generally produced by ellipsoidal benign lesions placed asymmetrically respect to axis of compression. Theoretically, it expecting observes a lack of fill-in for malignant cases due its spiculated shape that produces a firmly bounded condition. However, in-vivo studies have shown the presence of false fill-in when external compression is applied non-uniaxially over certain ultrasound probe-angle. In this paper we present an experimental and numerical study of fill-in behavior as function of the ultrasound probe angle and level of pre-compression for extreme bounding conditions that pretend to elucidate the nature of bonding. Results shows that for the case of firmly bounded inclusion the numerical model is similar to experimental estimation, but both show the lack fill-in signatures as product of large ultrasound probe angle. For loosely bounded inclusions, the experimental results differ from simulation and show that in general the bonding condition must be a complex function of the deformation or stress around the inclusion.

I. INTRODUCTION

INTRODUCCION DEL PROYECTO. REVISAR, ACTUALIZAR Y CONTEXTUALIZAR Breast cancer is the most common cancer among women worldwide and the second most common cancer overall. There are almost 1.7 million new cases diagnosed in 2012 (25% of all cancers in women) [6]. Breast cancer is the fifth cause of death from cancer overall (522.000 deaths). In developed regions it is the second cause of death after lung cancer (198.000 deaths, 15.4%) and it is the most frequent cause of cancer death in women in less developed regions (324.000 deaths, 14.3%) [6]. The rate of mortality (estimated age-standardized cases per 100.000) varies between regions in the range of 6 to 20 due to favorable survival rate in more developed regions [6]. In Chile, mortality rate rises up to 14.5 per 100.00 women in 2008, with a tendency to increase with age after 45 years, reaching a rate of 41.8 and concentrating 90.6% of all deaths [7]. This last fact is relevant if we consider that 68% of women older than 45 years did not undergo any medical examination (Casen 2011, [14]).

The most common method of breast cancer diagnosis is mammography, with a sensitivity of 67.8% and an accuracy of 70% [8]. However, sensitivity drops from 100% in fatty breast to about 45% in extremely dense breasts affecting more to younger patients, where cancer therapies are more effectives [8]. Other imaging methods like Magnetic Resonance Imaging (MRI) and Ultrasound Imaging (US) are often utilized to complement mammography [8]. MRI is highly sensitive [9-10] for detecting invasive breast cancer but less specific [11-12] compared to mammography. Moreover, due to long imaging times, high costs, and patient claustrophobia, only the 57.9% of the patients with high risk of breast cancer agree to undergo MRI screening after mammography and US [13]. For this reason US imaging (B-mode) has emerged as a useful, real-time and low-cost imaging modality in the detection of suspicious masses. Typically, it is used to differentiate between solid and cystic masses and to guide biopsy procedures. However, US imaging is highly operator dependent and it is only used as a supplementary method. Some sonography features based on the qualitative aspects of the shape, contour, margin and echogenicity, have been proposed for classifying breast tumors. However, the variability among observers has been a relevant and limiting issue to achieve a general consensus in the interpretation of these sonographic features [18-19]. In order to reduce operator dependence, an automated breast ultrasound technology (ABUS) has been approved by the FDA for screening hidden lesions in dense breast masses with negative mammogram [41]. In general, the uncertainties in imaging diagnosis have led to perform a high number of biopsies from which 75% (annually about 1 million) of them have had benign diagnosis [1]. This fact has become a considerable social-economic burden for the healthcare system. Therefore, any new imaging technology that may improve the accuracy of non-invasive differentiation between benign and malignant breast tumors will contribute positively to reduce cost and morbidity associated with unnecessary biopsies.

The Quasi-static Ultrasound Elastography (QUE) technique uses conventional sonographic images to visualize local tissue deformation when an external compression is applied by the ultrasound probe itself during the handheld ultrasonic scanning [14-26]. It aims to provide a better visualization of tumoral lesions than the conventional sonography, which are in general stiffer than the surrounded tissue [15]. In this context, the principle of the QUE technique comes from the manual palpation exam, where the healthcare specialist compresses the tissues in order to detect a suspicious object. From the physical point of view, the QUE technique considers that under a small (about 1-2%) quasi-static compression, the tissue behave as a linearly elastic solid, allowing to associate tissue deformation images with stiffness distribution [16]. The quasi-static character is guaranteed by the frame rate of the imaging system and the level of compression depends on the expertise of the operator. Generally, the QUE modality most used is the Axial Strain Elastogram (ASE) imaging, which is the strain tensor component along the axis of insonification [17]. This modality uses the high resolution property of ultrasonic images along the axial direction to generate ASE images of high quality. This is a direct consequence of the RF characteristics of ultrasonic signals that allow the tracking of tissue deformation by matching the stationary speckle pattern produced by the interaction between tissue heterogeneities with ultrasonic waves [17]. Also, this modality does not require specialized hardware modifications of the ultrasound machine allowing to capitalize the advantages of conventional ultrasound imaging technologies (non-invasive, non-ionizing, real-time and low cost). Clinical application of ASE imaging in breast tumor classification has been studied by several groups [20-24, 26]. In most of these reports, some features based on size discrepancy between the sonographic and elastographic tumor appearance, including strain contrast measures, have been used to differentiate benign from malignant tumors. However, the success of ASE differs from one study to other. In a meta-analysis of 22 clinical studies [27] it is shown that ASE sensitivity and specificity varied from 40% to 95%, in terms of biopsy results. This lack of consensus is attributed to low confidence on image interpretation, because ASE only offers contrast imaging improvements associated to stiffness changes between the lesion and the underlying tissue. This problem was addressed in a recent study [28], where a virtual simulation platform was built to validate the use of QUE methods in breast tumor diagnosis. Currently, ASE image modality is available in many commercial clinical US machines, but the lack of consensus among the clinical community and high dependence on the operator expertise has limited their use in the breast tumors diagnosis.

ASSE imaging is a QUE modality that gives information about the bonding condition of tumoral lesions with the

surrounding tissue. In breast tumor diagnosis the development of ASSE images was motivated by the fact that benign lesions (particularly fibrodenomas) are mobile because they are loosely-bonded to their surrounding tissue, whereas maligning tumors (cancers) are less mobile because they are firmly-bounded to their surroundings [32]. Due to the well-known lateral resolution limitations of US scanning technologies, the ASSE image only uses axial information of the Total Shear Strain Elastogram (TSSE, Equation 1). Initially, it has been showed that the ASSE image is directly influenced by the bonding condition at the inclusion-background boundary by using simulations, gelatin-phantom experiments, and in-vivo breast lesions [29-31]. Results from these studies have been very promising in breast tumor classification and have been corroborated by other research groups [4, 33-35]. Using the normalized axial shear strain area (NASSA, Figure 2), in vivo studies [31] have shown that the Receiver Operating Characteristic (ROC) curve is improved by a combination of NASSA plus BI-RADS (Breast Imaging Reports and Database System) scores in comparison with BI-RADS scores alone. However, these studies consider breast tumors as circularly-symmetric inclusions.

The rotation fill-in signature comes from an extension of the assumption of circularly-symmetric to elliptical non-normally oriented inclusions for benign breast lesions, which was motivated by the fact that fibroadenomas are known to be wider-than-taller in sonographic appearance [36,37]. In this context and by considering that benign breast lesions tend to be loosely-bonded to host tissue, the fill-in pattern is a manifestation of a slipping or rotation of the lesion produced by the asymmetrical stress distribution around the lesion. This asymmetry is introduced by non-normally orientation of the benign lesion respect to the axis of compression [2, 3]. In counterpart, malignant (cancers) breast lesions tend to be firmly-bonded to host tissue due to their irregular or spiculated shape, which avoids rotation under compression. As a consequence, the fill-in pattern is a signature of benignity, and then it could be used as a tool for non-invasive breast tumor classification [2-5]. However, the ASSE image only uses the axial information of tissue deformation (Equation 1), which limits the access to the lesion rotation. Moreover, the ASSE image is very sensitive to shearing features from surrounding tissue, which makes difficult its correct interpretation (Figure 1). To reduce these disadvantages, we can compute the rotational [39] (Equation 2) to generate an effective image of the lesion rotation, denominated Rotation Elastogram (RE) [36]. However, the incorporation of Lateral Shear Strain Elastogram (LSSE) increases the noise in the RE images. In this context, recent studies using beam-steering and synthetic transmit aperture (STA) methods have shown that the noise in the RE images can be significantly reduced improving the quality of the fill-in pattern signature [36, 54] (Figure 3). In addition, the ASSE image is very sensitive to the transducer-to-compression angle inducing the formation of false fill-in patterns. In this context, previous works have introduced the Rotation filter [37-38], as a measure of the transducer angle respect to the axis of compression. The use of the Rotation filter and an appropriate ASSE image segmentation and normalization may improve the fill-in pattern for in-vivo breast lesions screening [40, 42]. However, the Rotation filter is an indirect measurement of the transducer angle computed from the deepest part of axial displacement image, which is generally noisy due to lesion shadows.

II. MATERIALS AND METHODS

A. Experimental Setup

On Figure 1(a) is shown the experimental setup formed by a motorized linear translation stage (MODELO) with a rotation stage (ThorLab) controlled manually through a micrometer screw. The ultrasound linear array probe (Terason 12L5-V) is fixed into an acrylic box attached to the rotation stage and rotated until $\alpha \approx 10^o$. For each angle α, an uniform axial compression $\epsilon_0 \approx 1.5$ is applied by the translation stage using a compression plaque of $70x50mm$ appropriately mounted at bottom part of the acrylic box. The translation stage is also used to apply different levels of pre-compression $\epsilon_p = -(W/2L)\tan(\alpha)$ to avoid the lost of contact between the probe and the tissue mimicking phantom due to the rotation $x\tan(\alpha)$. The ultrasound machine Terason T3000 Avanced controlled by Matlab is used to acquiring the rf-raw data in quasi-static fashion and in synchronism with the applied axial compression ϵ_0 for each angle α of the ultrasound probe. This static angle is measured by an inertial sensor with 9 degree-of-freedom (IMU...MODELO) mounted on the acrylic box with the gravitational force along the a_x sensor, which gives $\alpha = \arctan\left(a_y/\sqrt{a_y^2 + a_z^2}\right)$. The cine-loop of ultrasonic data were acquired before, during and after the axial compression.

The tissue-mimicking phantoms were performed by pouring 5% of glass beads of $75\mu m$ of diameter into gelatin-distillated-water mixture at 45^oC, prepared before by pouring 5% of w/c of gelatin type B (Sygma Aldrich, bloom ≈ 225) into $600mL$ of distillated water at 75^oC. After to pour the glass beads, the gelatin mixture is placed into an rectangular mold of $106x100x50mm$ appropriately sealed, which in order to assure a homogeneous distribution of scatters (glass beads) was mount into a rotatory system until its solidification. The elliptical hard inclusions were

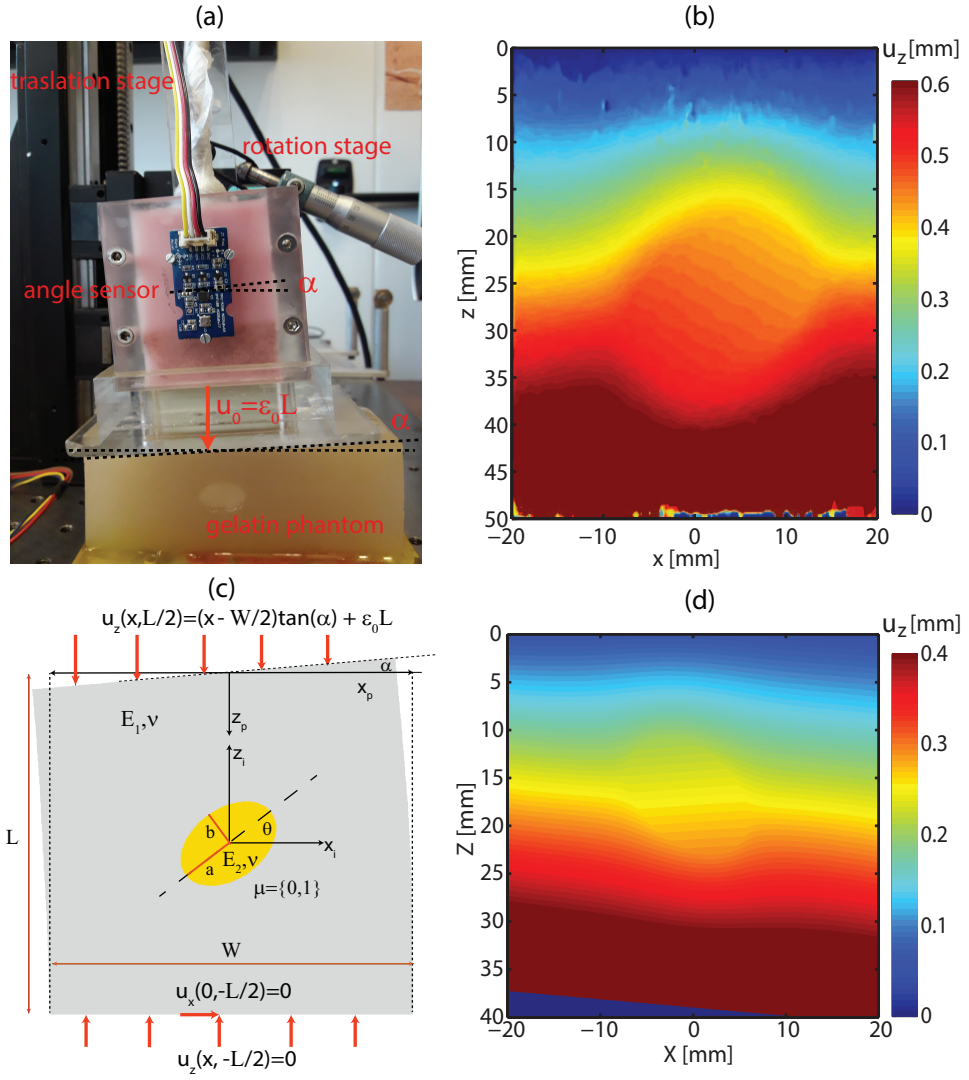

FIG. 1. (a) Experimental setup showing the traslation stage which allows applied the axial-strain $\epsilon_0 \approx 1.5\%$ at different angles of the ultrasound probe α by using the rotation stage. (b) Experimental axial displacement images u_z for an elliptical firmly bounded and inclined inclusion at $\theta \approx 45^o$ for $\alpha \approx 2^o$. (c) Boundary conditions for FEM simulations; rotation $x\tan(\alpha)$, axial traslation $-W\tan(\alpha)$ (pre-compression), uniaxial applied strain ϵ_0 and constraints at the bottom. (d) Simulated axial displacement images u_z for an elliptical firmly bounded ($\mu = 1$) and inclined inclusion at $\theta = 45^o$ for $\alpha = 4^o$

performed is similar fashion using ABS plastic molds fabricated by a 3D printer and impermeabilized by enamel paint. Two molds were fabricated; a cylinder of mayor radius $b = 8mm$, minor radiur $a = 5mm$ and $106mm$ of length and a rectangular mold with a cylindrical hole of slightly inferior size. The first ABS mold was fixed inside the rectangular mold and used to create the hole inside the rectangular soft phantom. The second ABS mold was used to pour a gelatin- distillated-water mixture of 15% of w/c and 5% of glass beads to create a loosely-bonded hard elliptical inclusion. For firmly bonded inclusion, the same gelatin mixture was pour into the elliptical hole performed previously in the rectangular phantom to glue the soft inclusion to surrounding soft media.

The axial displacement images (Figure 1(b)) are computed by a multilevel, coarse-to-fine, 2D block-matching algorithm described previously in [Thittai2010]. This is similar to those presented in the literature [Zhu2002, Shi2007, Lopata2009]. The principal difference was the use of the sum square difference (SSD) similarity measure in the coarse level on the envelope of the signal, followed by the cross-correlation (CC) measure on the RF signal in the fine level around the SSD-tracked coarse displacement region. The axial displacement images are computed between the average ultrasonic data captured before and after the axial compression ϵ_0 and in relative fashion for the rf-raw data captured during the compression. After tracking displacement procedure, the Axial strain and Axial-shear strain elastogram (ASE and $ASSE$ images) were generated by the staggered strain estimation [Srinivasan2002]. We are aware about

the rotation elastogram is more appropiated for fill-in studies, but our ultrasonic system does not allow to implement any method, as beam-sterring, to enhance the lateral resolution of the displacement images to improve the quality of the lateral component of the shear strain.

The $ASSE$ fill-in is computed from $ASSE$ images by filtering the outside region of the inclusion using a binary filter defined from the ASE images and improved by morphological operations. First, an ASE binary image is defined by an appropriate strain threshold $\approx 0.5ASE_{max}$, . Then, morphological operations are applied to reduce the size of the different objects producing its disconnection. Finally, a morphological filter is used to leave only the biggest object (inclusion) and its size is return back. The ASSE fill- in is then defined by Eq. 1:

$$ASSE_{fillin} = \frac{\overline{|ASSE|}_{inside}}{|ASSE|_{max}} \tag{1}$$

The ASE_{max} and $ASSE_{max}$ values are computed as the average of the top 50% and 5% pixels in the ASE and ASSE images respectively by using the correlation image (CC) as binary filter (pixels over 0.75) to avoid the bad estimated elastographic data.

B. Parametric Finite Elements Study

Parametric plane-strain (2D) finite elements simulations (FEM) were performed in ANSYS software (INFO) controlled by Matlab ambiance by using the APL commands. As geometrical model, we used a square domain of $L = W = 50mm$ with an elliptical inclusion of major axis $a = 8mm$ and minor axis $b = 4$ placed a the origin of coordinated system with its major axis rotate at angle θ respect to x-axis (see Figure 1(c)). Both domains, background and inclusion, are considered as linear isotropic elastic materials with Young's modulus $E_1 = 40kPa$ and $E_2 = 80kPa$, and Poison's ratio $\sigma_1 = \sigma_2 = \sigma = 0.499$. As was described in previous studies [REFER], for the loosely bounded condition we used the contact manager, where a symmetric contact-pair with friction parameter $\mu = 0.001$ is introduced. In the case of firmly bounded inclusions the glue function is used instead a higher friction coefficient. Meshing refinements was used in the interface between the inclusion and the background in order to avoid bad strain estimation. The bottom line is axially constrained by $u_x(x, -L/2) = 0$ and its central node is fixed along the lateral direction $u_y(0, -L/2) = 0$ in order to avoid the lateral displacement of the model. Before to apply the axial strain compression ϵ_0 on the top line at $z_i = L/2$, a rotation $x\tan(\alpha)$ and compression $-(W/2L)\tan(\alpha)$ of the top line is applied in multistep of $\alpha = 0.5$ to avoid large deformation. In each step the node positions are updated and the final step is used as the pre-node position. The axial compression is then applied and the node position are updated to define the post-node position. Both, pre and post-node position are exported to Matlab ambiance and used in the axial displacement computations (Figure 1(d)). The ASE and $ASSE$ images are computed from displacements images by using the gradient operation and the $ASSE$ fillin is estimated in the fashion than the experimental data.

III. RESULTS

A. Ultrasound probe angle behavior

B. Pre-compression behavior

IV. CONCLUSIONS

Results shows that for the case of firmly bounded inclusion the numerical model is similar to experimental estimation, but both shows the lack fill-in signatures as product of large ultrasound probe angle.

V. ACKNOWLEDGMENTS

DICYT-Usach 041731GD is acknowledged for support. Authors are grateful to .... for valuable help.

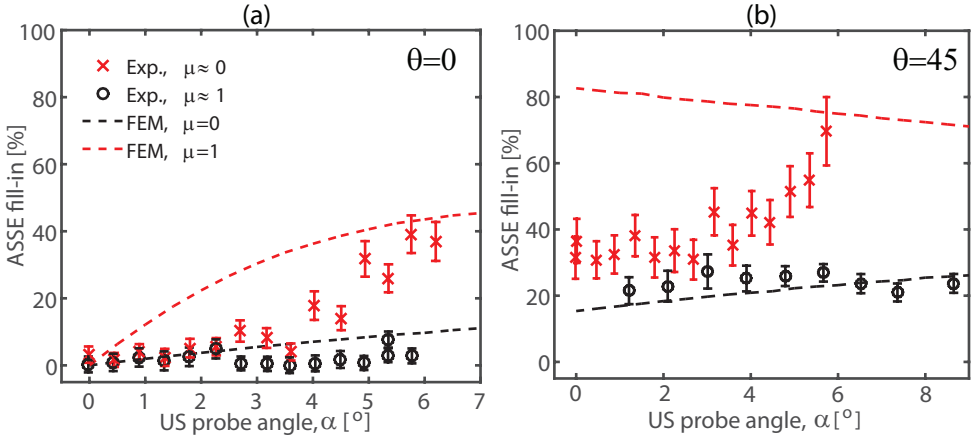

FIG. 2. Axial-shear strain fill-in at different angles of the ultrasound probe α for firmely and loosely elliptical inclusions (red and back symbols). Segmented lines represent the results from parametric FEM simulations. (a) Non-inclined inclusions $\theta \approx 0^o$. (b) Inclined inclusions $\theta \approx 45^o$. The pre-compression level is about 8% corresponding to angle $\alpha \approx 7^o$.

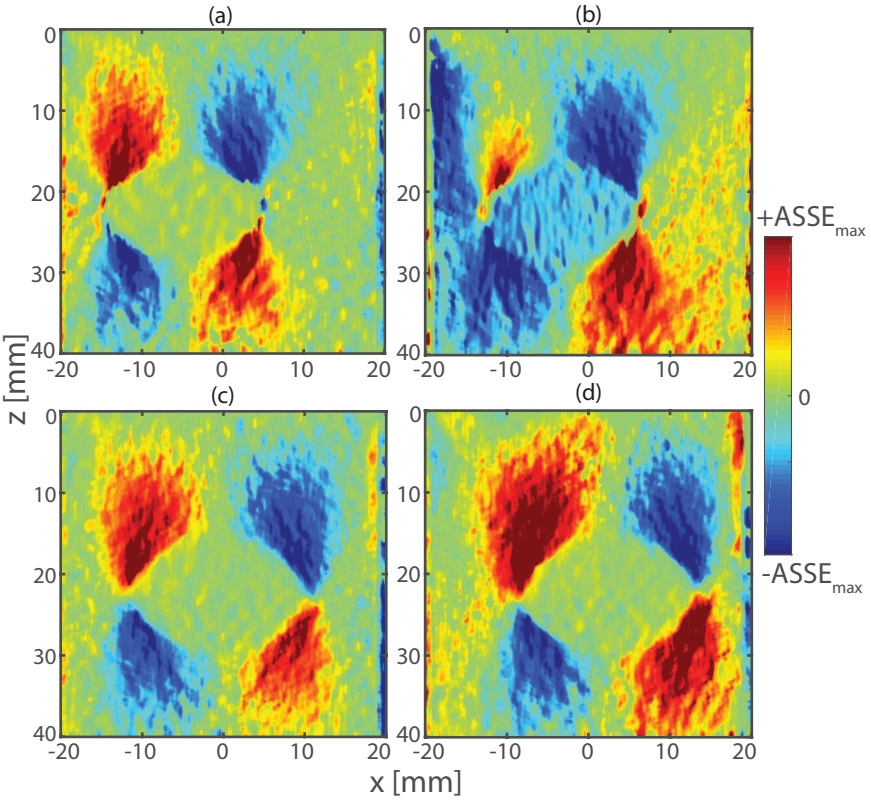

FIG. 3. Experimental ASSE images for extremes ultrasound probe angles ($\alpha = 0$ and 6^o) of the results shown in 2(a). (a,b) Non-inclined loosely bounded inclusion. (c,d) Non-inclined firmly bounded inclusion.

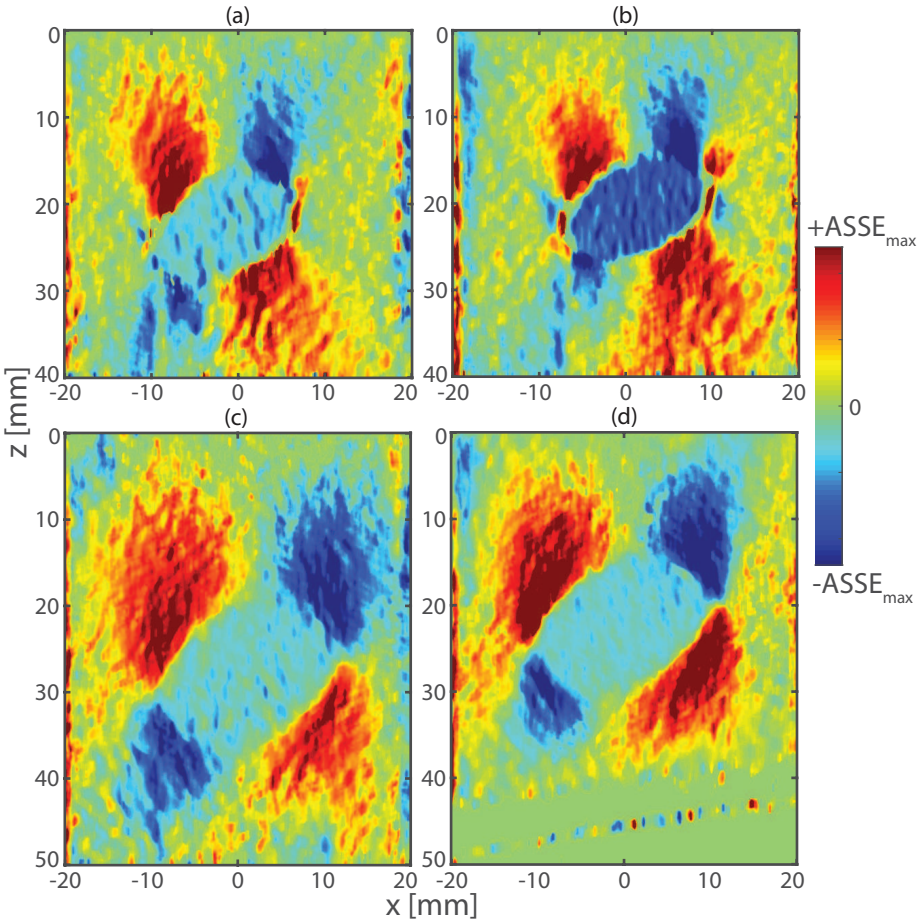

FIG. 4. Experimental ASSE images for extremes ultrasound probe angles ($\alpha = 0$ and 6^o) of the results shown in 2(b). (a,b) Inclined ($\theta \approx 45^o$) loosely bounded inclusion. (c,d) Inclined ($\theta \approx 45^o$) firmly bounded inclusion (lack of false fill-in).

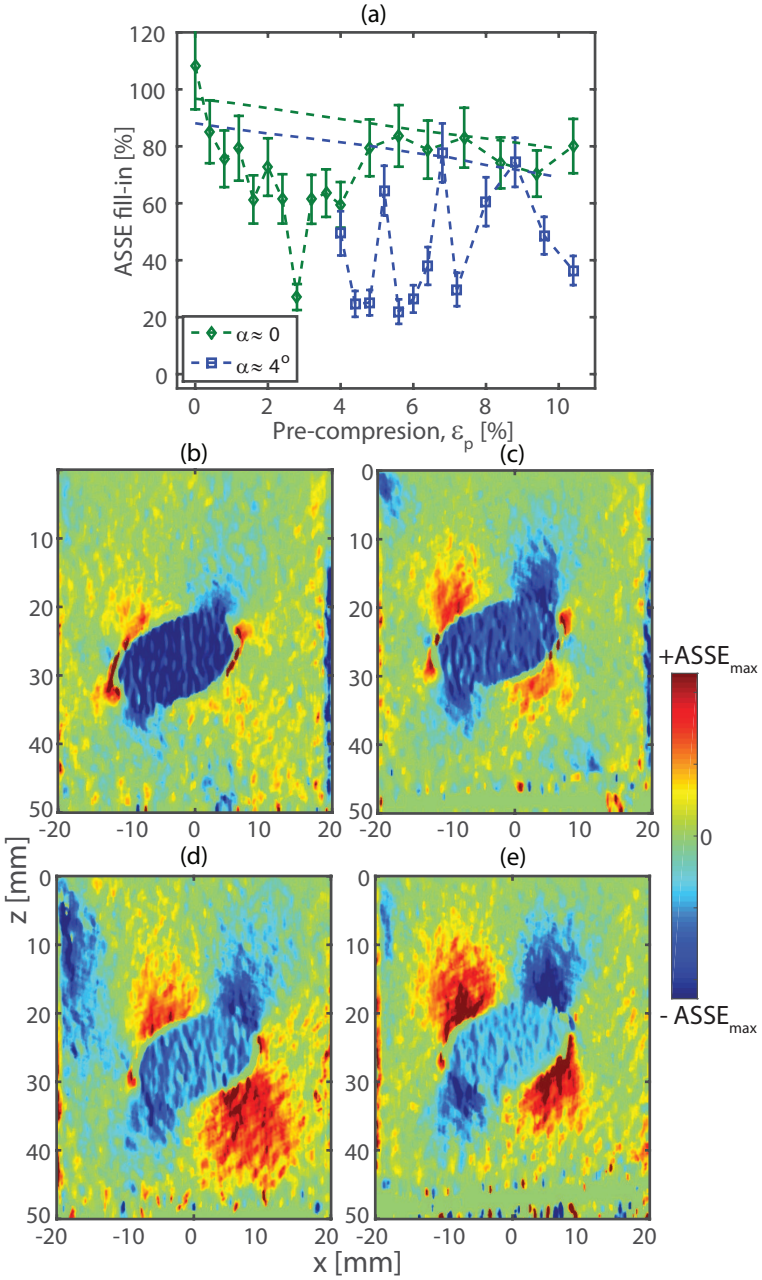

FIG. 5. (a) Axial-shear strain fill-in at different levels of uniaxial pre-compression for a loosely bounded inclined ($\theta \approx 45^o$) elliptical inclusion. Experiment perfomed for two angles of ultrasound probe $\alpha = 0$ and 4^o (red and blue symbols). Segmented lines represent the results from parametric FEM simulations. (b) Experimental ASSE image for $\alpha = 0$ at 0% of pre-compresion.(c) Experimental ASSE image for $\alpha = 0$ at $\epsilon_p = 8\%$ of pre-compresion. (d) Experimental ASSE image for $\alpha = 4^o$ at $\epsilon_p = 4\%$ of pre-compresion.(e) Experimental ASE image for $\alpha = 4^o$ at $\epsilon_p = 9.5\%$ of pre-compresion.